ACS OMEGA

http://pubs.acs.org/journal/acsodf

Article

Ligand Degradation Study of Unsymmetrical β-Diketiminato Copper Dioxygen Adducts: The Length Chelating Arm Effect

Kuldeep Chand, Naorem Jemes Meitei, Yu-Lun Chang, Cheng-Long Tsai, Hsing-Yin Chen,* and Sodio C. N. Hsu*

Cite This: *ACS Omega* 2023, 8, 21096−21106

Read Online

ACCESS | Metrics & More | Article Recommendations | Supporting Information

ABSTRACT: An investigation on the reactivity of O_2 binding to unsymmetrical β-diketiminato copper(I) complexes by spectroscopic and titration analysis was performed. The length of chelating pyridyl arms (pyridylmethyl arm vs pyridylethyl arm) leads to the formation of mono- or di-nuclear copper-dioxygen species at −80 °C. The pyridylmethyl arm adduct ($\mathbf{L_1CuO_2}$) forms mononuclear copper-oxygen species and shows ligand degradation, resulting in the formation of (2*E*,3*Z*)-*N*-(2,6-diisopropylphenyl)-4-(((*E*)-pyridin-2-ylmethylene)amino)pent-3-en-2-imine, which slowly converts to its cyclization isomer 1-(2,6-diisopropylphenyl)-4,6-dimethyl-2-(pyridin-2-yl)-1,2-dihydropyrimidine after addition of NH_4OH at room temperature. On the other hand, the pyridylethyl arm adduct $[(\mathbf{L_2Cu})_2(\mu\text{-O})_2]$ forms dinuclear species at −80 °C and does not show any ligand degradation product. Instead, free ligand formation was observed after the addition of NH_4OH. These experimental observations and product analysis results indicate that the chelating length of pyridyl arms governs the Cu/O_2 binding ratio and the ligand degradation behavior.

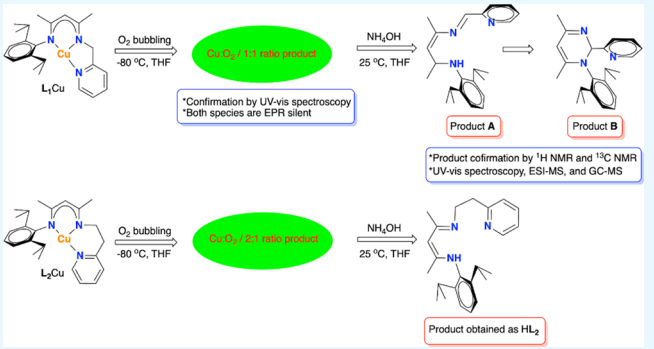

INTRODUCTION

Investigation on copper dioxygen adducts has attracted attention due to their role in bioinspired chemistry and catalysis since they have a strong resemblance to the oxidation and oxygenation reactions in biotic as well as in the material industry.[1−8] These adducts can exist as mononuclear and dinuclear forms, which are influenced by ligand denticity, intramolecular hydrogen bonding, and electronic and steric effects of the supporting ligands.[9−18] The reaction of copper(I) complexes with O_2 at a 1:1 copper/dioxygen ratio (Scheme 1) resulted in the formation of mononuclear copper dioxygen adducts such as copper(II)-superoxo ($^{E}\mathbf{S}$ and $^{S}\mathbf{S}$) and copper(III)-peroxo ($^{M}\mathbf{P}$) complexes.[3,6,19−23] On the other hand, dinuclear copper dioxygen adducts could be formed by entrapping another copper(I) complex from mononuclear copper dioxygen adducts with a 2:1 copper/dioxygen ratio, which exist as copper(II)-end-on peroxo ($^{T}\mathbf{P}$), copper(II)-peroxo ($^{S}\mathbf{P}$), and bis(μ-oxo)di-copper(III) complexes ($\mathbf{O}$) binding modes.[24−28]

The reaction of symmetrical *N*,*N*′-aryl β-diketiminato copper(I) complexes with O_2 gives mono- and/or di-copper dioxygen adducts and has been well documented,[29−35] and the role of substitutions is summarized in Scheme 2a. The isolation of mono-copper dioxygen adducts only achieved on the reaction of steric-hindered *N*,*N*′-aryl β-diketiminato copper(I) complexes with O_2,[2,4,29−31,36−38] while less hindered copper(I) variants form bis(μ-oxo)copper(III) products.[2,8] Apart from it, the thioether arm of unsymmetrical *N*,*N*′-aryl β-diketiminato mono-copper dioxygen adduct would be able to trap another copper(I) complexes and led to bis(μ-oxo)copper product formation, which was observed upon removal of O_2 by purging with argon (Scheme 2b).[4]

The reactivity of the β-diketiminato Cu/O_2 adducts was reported to be dependent on temperature, solvent, and concentration, which makes characterization difficult.[30] Tolman et al. reported that the β-diketiminato Cu/O_2 (1:1) adduct is a poor oxidant by examining its reactivity with a range of H-atom donors including phenols.[36,39] Upon addition of phosphine to this Cu/O_2 (1:1) adduct, no phosphine oxide was produced, resulting in loss of O_2 and the formation of Cu(I) phosphine adducts. However, isolation of Cu(II)-*o*-iminosemiquinonato species indicates that the reactivity of the β-diketiminato Cu/O_2 (1:1) adduct might induce the hydroxylation and rearrangement aryl group of the ligand.[39] Taking advantage of the dioxygen activation of *N*,*N*′-aryl β-

Received: March 27, 2023
Accepted: May 12, 2023
Published: May 26, 2023

Scheme 1. Representation of Superoxo, Peroxo, and Bis(μ-oxo) Copper Cores

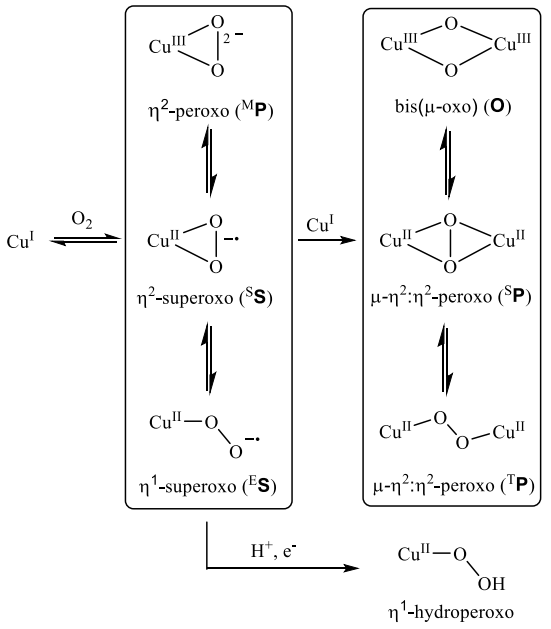

diketiminato copper(I) complexes mentioned above, the ligand steric factor and copper/dioxygen ratio (1:1 or 2:1) play important roles in mono-/di-copper dioxygen complex formation.[2,4,8,29−31,36−38] In contrast to *N*,*N*′-aryl-substituted analogues, a dioxygen activation study on the *N*-aryl-*N*′-alkylpyridyl unsymmetrical *β*-diketiminato copper(I) complexes was lacking. The study on the *N*-aryl-*N*′-alkylpyridyl unsymmetrical *β*-diketiminato copper(I) complexes $\mathbf{L_1}$Cu or $\mathbf{L_2}$Cu shows that the length of the pyridyl arm will affect the reactivity of small molecules such as carbon monoxide binding to the copper center.[40] Therefore, the importance of the length of the pyridylalkyl arm in unsymmetrical *β*-diketiminate ligands[40−42] inspired us to further check the reactivity of *N*-aryl-*N*′-alkylpyridyl *β*-diketiminato copper(I) complexes with O_2 (Scheme 2c).

RESULTS AND DISCUSSION

Room-Temperature Examinations of Copper(I) Complexes with Dioxygen. The reactions of $\mathbf{L_1}$Cu or $\mathbf{L_2}$Cu ($\mathbf{L_1}$ and $\mathbf{L_2}$ are defined in Scheme 2c) with O_2 had been examined in MeOH and MeCN, in which only $[(\mathbf{L_2}Cu)_2(\mu\text{-}OH)_2]$ was isolated as a crystalline solid.[40] However, the treatment of $\mathbf{L_1}$Cu with O_2 resulted in the formation of copper(II) products that could not be characterized in pure form. Based on these observations, we further studied the reaction of $\mathbf{L_1}$Cu or $\mathbf{L_2}$Cu with O_2 in THF at ambient temperature, which produced green solutions, indicating the formation of copper dioxygen adducts as Cu(II) species. Significant UV−vis changes were observed, however, due to unstable and highly reactive natures of the copper dioxygen adducts, making these species difficult to isolate at ambient temperature.

Low-Temperature Examinations of Copper Dioxygen Adducts. To get further information about copper dioxygen adducts, it was quite necessary to check the reaction conditions at low temperatures. Examinations of the $\mathbf{L_1}$Cu or $\mathbf{L_2}$Cu toward dioxygen at −80 °C in THF resulted in the growth of new features in the UV−vis spectra (Figure 1); these absorptions were unperturbed upon removal of excess O_2 but bleached upon warming. More importantly, the monitoring of copper dioxygen species resulted in a decreased peak at ∼350 nm for $\mathbf{L_1}$Cu ($\varepsilon \sim 9500$) (Figure 1a) along with a less intense broad feature at ∼600 nm. In the case of $\mathbf{L_2}$Cu ($\varepsilon \sim 4926$) (Figure 1b), a new peak formation at 430 nm was observed. Low temperature titration results clearly confirm the formation of $\mathbf{L_1}Cu/O_2$ in 1:1 ($\mathbf{L_1}CuO_2$) and $\mathbf{L_2}Cu/O_2$ in 2:1 $[(\mathbf{L_2}Cu)_2(\mu\text{-}O)_2]$ stoichiometry.

The UV−vis absorption features degrade upon the solutions returned to room temperature, indicating the formation of thermally unstable copper dioxygen adducts (Figure S1). A reversible dioxygen binding behavior of *N*,*N*′-aryl *β*-diketiminato Cu/O_2 (1:1) adduct has been reported and promoted by its thioether arm, which will also facilitate trapping of the generated Cu(I) species to reform the bis(*μ*-oxo) di-copper(III) adducts (Scheme 2b).[4] However, these reversible O_2 binding behaviors were not observed in our examinations of $\mathbf{L_1}$Cu or $\mathbf{L_2}$Cu complexes with O_2, which may contribute by the pyridylalkyl arm of ligand. On the other hand, no scrambling results were observed when $\mathbf{L_2}$Cu was added to the $\mathbf{L_1}CuO_2$ species solution, indicating the unique reactivity of *N*-aryl-*N*′-alkylpyridyl unsymmetrical *β*-diketiminato copper(I) complexes ($\mathbf{L_1}$Cu and $\mathbf{L_2}$Cu) in comparison with *N*,*N*′-aryl *β*-diketiminato copper(I) complexes. The final product obtained is only the formation of mono-copper dioxygen adduct $\mathbf{L_1}CuO_2$, as indicated by the UV−vis titration results and the comparative spectral features with other symmetrical *N*,*N*′-aryl *β*-diketiminato copper precedents.[2,4,29−31,36−38] To further confirm the formation of $\mathbf{L_1}CuO_2$ species, an independent synthesis was performed by treatment of $\mathbf{L_1}CuCl$[42] with KO_2/18-crown-6 to give $\mathbf{L_1}CuO_2$ species evidenced by UV−vis spectrum comparison with species from the reaction of $\mathbf{L_1}$Cu with O_2. On the other hand, alternative ways for the $[(\mathbf{L_2}Cu)_2(\mu\text{-}O)_2]$ species were achieved by the reaction of $\mathbf{L_2}CuCl$[42] with H_2O_2/Et_3N, which shows a similar absorption pattern in the UV−vis spectrum observed by the reaction of $\mathbf{L_2}$Cu with O_2 (Figures S2 and S3).[9,43] The $\mathbf{L_1}CuO_2$ and $[(\mathbf{L_2}Cu)_2(\mu\text{-}O)_2]$ species both are EPR-silent (Figure S4). The EPR silence of dioxygen activation species, such as $\mathbf{L_1}CuO_2$ and $[(\mathbf{L_2}Cu)_2(\mu\text{-}O)_2]$, can be attributed to their spin state, which is determined by the antiferromagnetic coupling of the unpaired electrons associated with copper(II) and the superoxide ligand.[10] Spin triplet species with two unpaired electrons exhibit paramagnetic behavior, while spin singlet species with no unpaired electrons are diamagnetic.[10,44−47] Previous literature has shown that peroxo species are EPR-silent due to their diamagnetic nature, while superoxo species exhibit antiferromagnetic coupling behavior.[48,49]

To understand the formation of monomer/dimer type of copper dioxygen adducts, we conducted a literature survey of UV−vis spectral data, which is shown in Figures S1−S7 and Tables S1−S7,[3,6,19−22] and the *β*-diketiminato copper precedent binding modes are shown in Scheme 2. Although literature reports suggest the successive evolution of the copper(II)-superoxo ($^{E}\mathbf{S}$ and $^{S}\mathbf{S}$) to copper(III)-peroxo ($^{M}\mathbf{P}$) species,[21,22,50] the stoichiometric titration results of the $\mathbf{L_1}Cu/O_2$ (1:1) adduct at −80 °C show several shifts or intensity changes of the intra-ligand and charge transfer bands, along with a less intense broad feature at ∼600 nm, which are in agreement with UV−vis spectra features of the copper(II)-superoxo ($^{E}\mathbf{S}$) or copper(II)-peroxo ($^{M}\mathbf{P}$) precedents.[4,29−31,36−38] This comparison suggests that copper(II)-superoxo ($^{S}\mathbf{S}$) type of species formation at −80 °C is unlikely.

https://doi.org/10.1021/acsomega.3c02004
ACS Omega 2023, 8, 21096−21106

Scheme 2. (a) Illustration of the Manner in Which Steric Substituents Control the Development of Mono- to Di-copper Dioxygen Adducts; (b) Representation on the Dioxygen Reactivity of Thioether Substituent Effect of Monocopper Dioxygen and Di-copper Dioxygen Adducts; (c) in the Development of Mono- to Di-copper Dioxygen Adducts, the Length of the Pyridylalkyl Arm Plays an Important Role in the Cu/O_2 Ratio Stoichiometry

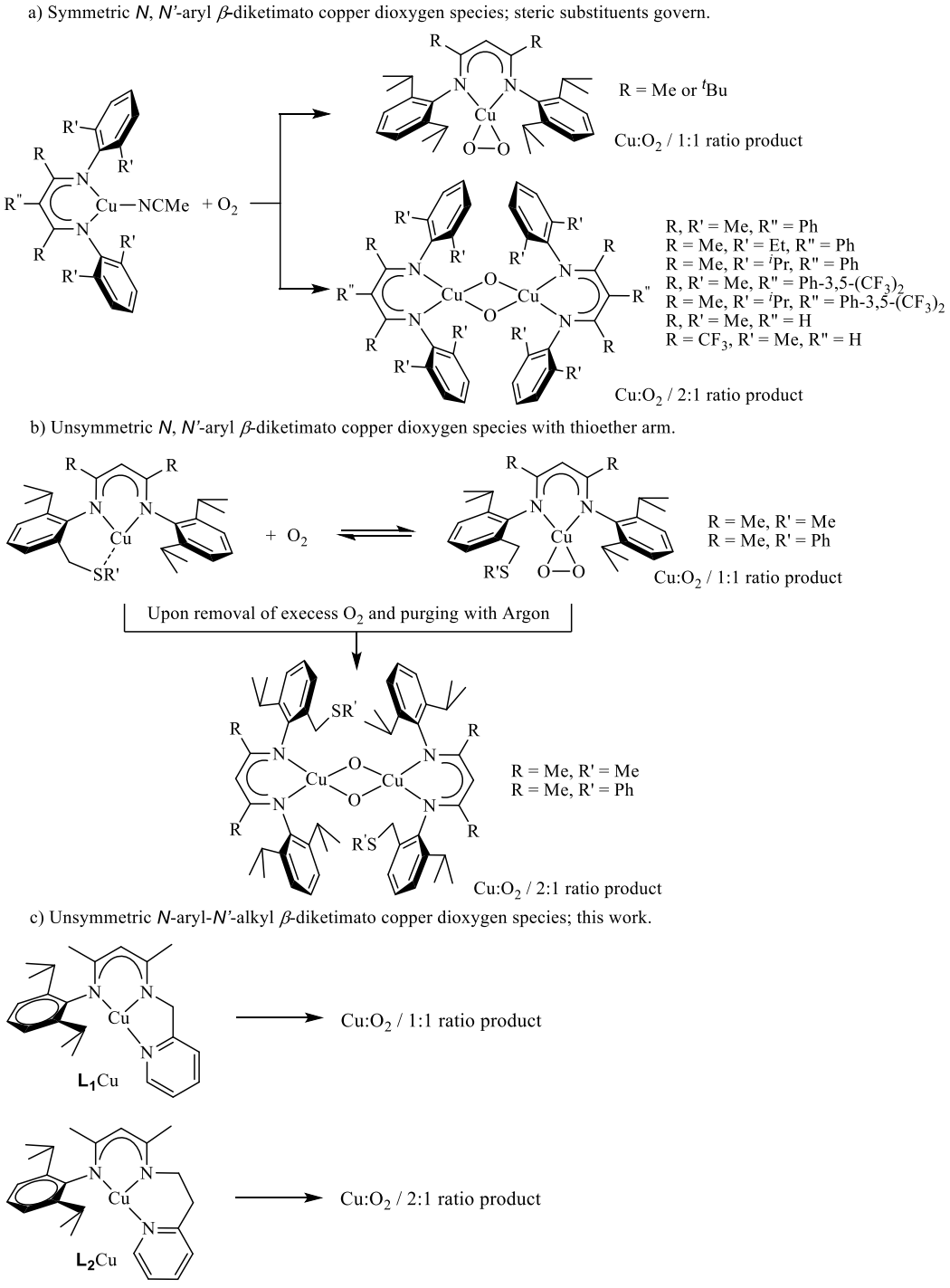

On the other hand, the stochiometric titration results of the $\mathbf{L_2}Cu/O_2$ (2:1) adduct reveal the development of the UV−vis absorption charge transfer band between 415 and 470 nm, which is also observed in the UV−vis spectra features of the 2:1 copper/dioxygen ratio bis(μ-oxo)dicopper(III) species (**O**) precedents (Table S6).[4,8] Despite several unsuccessful attempts to characterize the $\mathbf{L_1}CuO_2$ species by resonance Raman spectroscopy, we were only able to tentatively assign the possible binding mode of $\mathbf{L_1}Cu/O_2$ (1:1) adduct as copper(II)-peroxo (^{M}**P**) with the help of UV−vis features and EPR, by comparing it with the precedents of β-diketiminato copper dioxygen species.

Product Analysis with or without NH_4OH Treatment. The examinations of GC/MS analysis of the organic products of *N*,*N*′-aryl β-diketiminato copper dioxygen complexes were reported, which revealed the formation of over 25 different organic substances, which suggests that the ligand degradation or decomposition proceeds via multiple pathways and is not

https://doi.org/10.1021/acsomega.3c02004
ACS Omega 2023, 8, 21096−21106

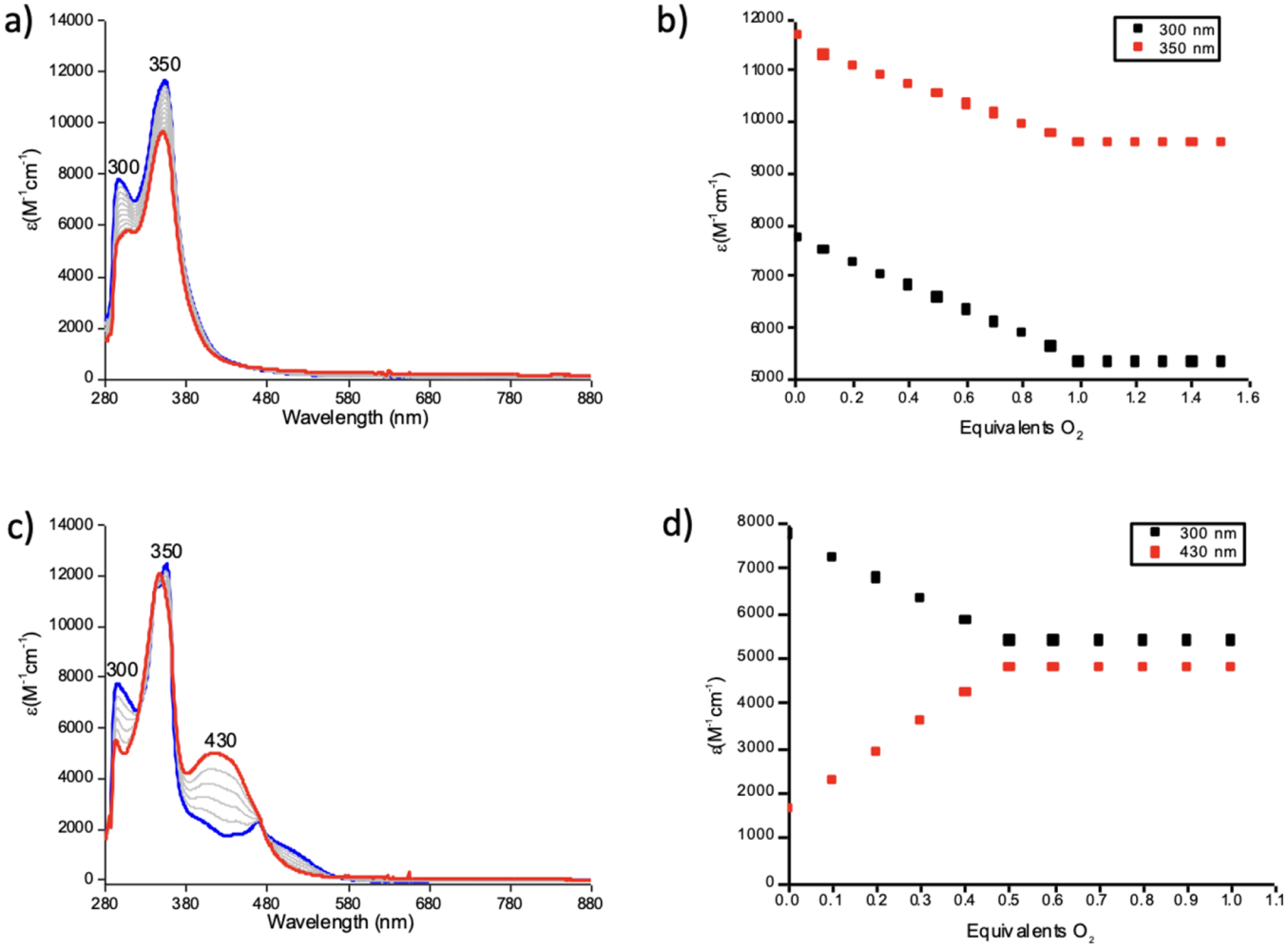

Figure 1. Titration results of O_2 saturated THF at −80 °C to L_1Cu (0.175 mM) (a) and (b). (c) and (d) Titration results regarding L_2Cu. Spectra represent before O_2 addition (blue) and after O_2 addition (red).

Scheme 3. Illustration of the Ligand Degradation Products A and B from the Reaction of L_1Cu with O_2

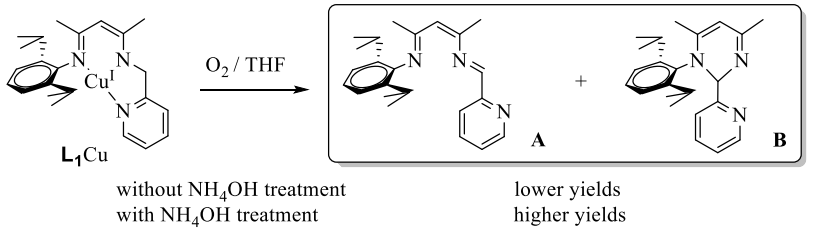

Table 1. Ligand Degradation Product Analysis of the Copper Dioxygen Complexes with Ammonium Hydroxide[a]

entry	complexes	oxygenation temperature/NH_4OH stirring time	product **A** %	product **B** %	ligand %
1	L_1Cu	25 °C/30 min	59.9 ± 0.5		
2	L_1Cu	25 °C/2 h		55.1 ± 0.9	
3	L_1Cu	−80 to 25 °C/30 min	70.1 ± 0.7		
4	L_1Cu	−80 to 25 °C/2 h		62.7 ± 0.2	
5	L_2Cu	25 °C/30 min			60.0 ± 0.8
6	L_2Cu	−80 to 25 °C/2 h			65.1 ± 0.7

[a]All reactions of copper complexes with dioxygen bubbled time was 30 min.

fully characterized.[30,39] We examined the reaction mixture of L_1Cu with O_2 at −80 °C; then warming to room temperature gives complicated results of organic substances. Inspired by precedent results of using NH_4OH as a demetallation agent,[7,51−55] a ligand degradation product study of L_1CuO_2 species in THF at −80 to 25 °C, following treatment of NH_4OH, allows us to isolate two sole products depending on reaction time (Scheme 3); a ligand degradation product

https://doi.org/10.1021/acsomega.3c02004
ACS Omega 2023, 8, 21096−21106

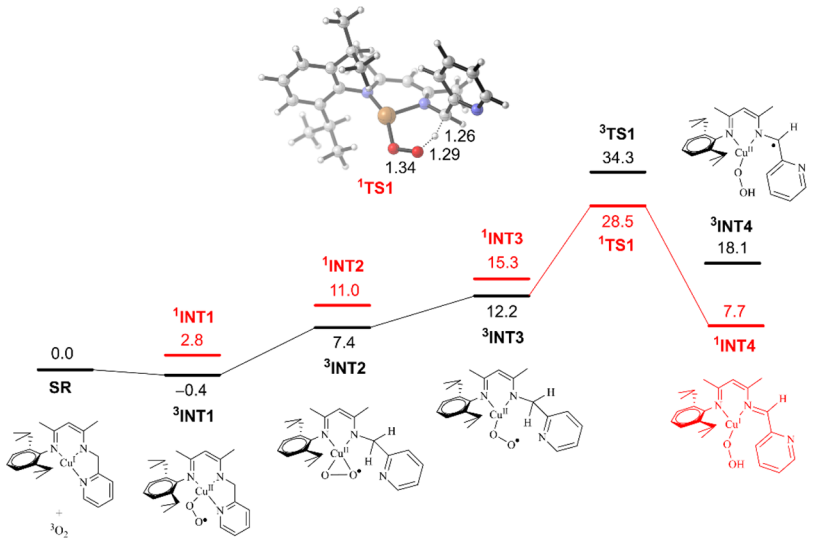

Figure 2. Free energy profile (in kcal/mol) for the reaction of L_1Cu and O_2.

(2*E*,3*Z*)-*N*-(2,6-diisopropyl phenyl)-4-(((*E*)-pyridin-2-yl-methylene) amino)pent-3-en-2-imine (**A**; 70.1 ± 0.7% yield) was isolated in 30 min. On the other hand, a cyclic product of 1-(2,6-diisopropyl phenyl)-4,6-dimethyl-2-(pyridin-2-yl)-1,2-dihydropyrimidine (**B**; 62.7 ± 0.2% yield, Table 1) was also isolated as a single product after 2 h. Due to the unstable nature of product **A**, we observe that the yields of product **A** gradually decreased and the yield of product **B** increased (see Tables 1 and S8) in 2 h, while in the case of $[(L_2Cu)_2(\mu\text{-}O)_2]$ species, no significant ligand degradation products were obtained, instead of free HL_2 isolated in 65.1 ± 0.7% yield.

The ligand degradation study of L_1CuO_2 species in THF at −80 to 25 °C without NH_4OH shows a lower yield of product in **A** in 30 min 20.1 ± 0.6% and **B** in 2 h (13.4 ± 0.6%; see Table S8). These results indicate the importance of NH_4OH addition as a demetallation agent for degradation product isolation. In order to consider how the temperature affects the product distribution, the yields of products **A** and **B** have been examined in the room temperature (25 °C) oxygenation experiments, followed by NH_4OH addition. A lower yield of products **A** and **B** was isolated from the room temperature oxygenation examinations, suggesting the thermal instability of species L_1CuO_2. Again, the study at 25 °C with NH_4OH shows 70.1 ± 0.7% of products **A** (30 min) and 62.7 ± 0.2% of **B** (2 h), while the study at 25 °C without NH_4OH shows 15.2 ± 0.6% of products **A** (30 min) and 10.0 ± 0.3% **B** (2 h). The lower yields of **A** and **B** were obtained when NH_4OH was absent, suggesting that the demetallation agent (NH_4OH) plays a role in the **A** and **B** formation. The addition of NH_4OH helps the yield of sole ligand degradation products **A** and **B**, which may imply the importance of the copper-mediated pathway in the dioxygen activation of copper species and the following ligand degradation process. The results obtained during the ligand degradation process help us to conclude that the whole process depends upon several factors such as temperature, reaction time, treatment of NH_4OH, and the length of pyridylalkyl arm.

In order to confirm the stability of product **A** and its conversion to product **B**, the independent synthesis of product **A** was performed from 2-pyridine carboxaldehyde and amine[56] in the presence of 5 Å molecular sieves as a catalyst.[57] The examination of product **A** converted to **B** in the presence of NH_4OH was monitored and confirmed by ^{1}H-NMR and UV−vis spectroscopy (Figures S24 and S25). During the NMR monitoring experiments, **A** slowly converts to **B**, as evidenced by increasing peaks of 2.9, 3.20, and 6 ppm. The complete disappearance of signals of **A** in 2 h confirms the full conversion of **A** to **B**.

In the case of $[(L_2Cu)_2(\mu\text{-}O)_2]$, free HL_2 was isolated in a lower yield of 20.1 ± 0.6% (30 min) in contrast to a higher yield of 65.1 ± 0.7% NH_4OH addition. At 25 °C, free HL_2 was isolated in a lower yield of 5.1 ± 0.1% as compared to a higher yield of 60.0 ± 0.8% with NH_4OH addition in 30 min (see Tables 1 and S8). The confirmation of the product was done with the help of NMR, ESI-MS, and GC−MS (Figures S12−S23).[58]

DFT Calculation. Density functional theory (DFT) calculations were performed to shed light on the pathway of dioxygen activation by L_1Cu and the following ligand degradation. The calculated free energy profile for the reaction of L_1Cu with O_2 is shown in Figure 2, and the analysis of charge and spin distribution for each structure is given in Tables S9 and S10.

Starting from separated reactants $L_1Cu + O_2$ (**SR**), the first step is an association to form the end-on superoxo complex **INT1**. The distance between terminal oxygen and methylene hydrogen in **INT1** is 5.29 Å, too far to undergo hydrogen atom transfer (HAT) from methylene group to superoxo. Prior to HAT, the chelating pyridyl arm has to open to form a four-coordinate side-on intermediate **INT2,** followed by trans-formation to a three-coordinate end-on intermediate **INT3**, in which the distance between terminal oxygen and methylene hydrogen is now 2.40 Å, ready to undergo HAT. The electronic ground states of superoxo complexes **INT1−3** are triplet states (the spin on Cu and superoxo is parallel); the singlet states (the spin on Cu and superoxo is anti-parallel) were found to be ca. 3 kcal/mol higher in energy than the corresponding triplet states. However, the calculations show that the singlet states of the following transition state of HAT **TS1** and the resulting hydroperoxo complex **INT4** become lower in energy than the corresponding triplet states, indicating that a spin crossover occurs in the course of HAT. In the singlet state pathway, the HAT from the methylene group to superoxo is concomitant with further oxidation of ligand by

https://doi.org/10.1021/acsomega.3c02004
ACS Omega 2023, 8, 21096−21106

Cu(II), that is, an electron transfer from ligand to Cu(II), leading to the formation of Cu(I) hydroperoxo complex ^{1}**INT4**. On the other hand, the corresponding process on the triplet state is a simple HAT that results in the formation of Cu(II) hydroperoxo complex ^{3}**INT4** with a significant spin density on the ligand (Table S9). The over energy barrier for the HAT reaction is 28.5 kcal/mol, indicating that the ligand degradation through this pathway is a slow process.

The high energy barrier for the HAT in the abovementioned pathway is, in part, due to additional energy cost for opening the pyridyl arm. An alternative pathway that can avoid this additional energy cost involves a bimolecular reaction of two superoxo complexes L_1CuO_2 (^{3}**INT1**), as shown in Figure 3.

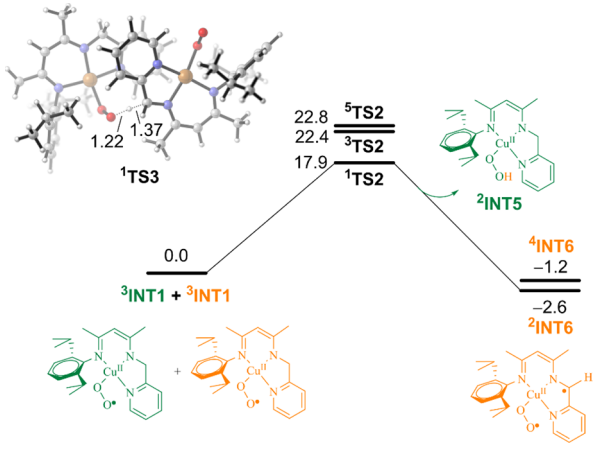

Figure 3. Free energy profile (in kcal/mol) for the bimolecular reaction of two L_1CuO_2.

In this pathway, the superoxo on one of the ^{3}**INT1** abstracts a hydrogen atom from the methylene group on the other ^{3}**INT1**, leading to the formation of a Cu(II) hydroperoxo complex ^{2}**INT5** and a Cu(II) superoxo complex ^{2}**INT6**. In contrast to the unimolecular reaction pathway, wherein the HAT is accompanied by an electron transfer from ligand to Cu(II) (^{3}**INT3** to ^{1}**INT4** in Figure 2), the intermolecular HAT in the bimolecular reaction pathway occurs without further oxidation of the anionic ligand, clearly evidenced by the substantial negative charge and spin density on the ligand in ^{2}**INT6** (Table S9). It appears that the further oxidation of the dehydrogenated ligand by Cu(II) is sensitive to the binding mode between them; it occurs at bidentate binding structures ^{1}**TS1** but not at tridentate binding structure **TS2**. This is probably because the tridentate binding mode induces a larger electron density shift from ligand to Cu(II) in comparison to the bidentate binding mode. The electron density shift from ligand to Cu(II) has two effects: on the one hand, it decreases the reduction potential and the oxidation ability of Cu(II); on the other hand, it stabilizes electronic energy levels on the ligand. This cooperative effect renders the electron transfer from dehydrogenated ligand to Cu(II) energetically unfavorable at tridentate binding mode. The **INT6** is expected to undergo ligand dissociation and electron transfer from dehydrogenated ligand to Cu(II) upon the addition of NH_4OH, leading to the formation of free two-electron oxidized ligand product **A**.

The energy barrier of HAT for the bimolecular reaction pathway (^{1}**TS2** in Figure 3) is 17.9 kcal/mol, considerably lower than 28.5 kcal/mol in the unimolecular reaction pathway (^{1}**TS1** in Figure 2). We would like to mention that there exists uncertainty for the low energy barrier estimated by ^{1}**TS2** as a result of substantial spin contamination detected in the broken-symmetry wavefunction for the open-shell singlet transition state ^{1}**TS2** (S^2 = 1.966). Nevertheless, given that the energy barrier derived from the quintet transition state ^{5}**TS2**, in which the spin contamination is negligible (S^2 = 6.027), is 22.8 kcal/mol, still lower than that of the unimolecular reaction pathway, one can conclude that the intermolecular HAT is the major pathway for ligand degradation.

Possible Pathway of Cu/O_2 Adduct Formation and Ligand Degradation. Based on the low-temperature UV−vis spectra, product examinations, and DFT calculation results, the dioxygen activation of L_1Cu and its ligand degradation pathway is shown in Scheme 4. Two molecules of superoxo ^{3}**INT1** species will react with each other to perform the intermolecular HAT without opening of the pyridyl arm and resulting in the formation of the hydroperoxo ^{2}**INT5** and superoxo ^{2}**INT6** species. The presence of NH_4OH as a demetallation agent will immediately produce ligand degradation products **A**. Another cyclization isomer **B** will appear as the reaction time increases.

Product **B** had been reported and observed as a ligand in complex [**B**Cr(CO)$_4$] (**B** = κ^2−1-(2,6-diisopropylphenyl)-4,6-dimethyl-2-(pyridin-2-yl)-1,2-dihydropyrimidine),[58] which was synthesized via CO-induced and chromium-mediated C−H activation on the methine-proton of methyl pyridyl arm of *N*-aryl-*N*′-alkyl unsymmetrical *β*-diketiminato ligand, followed by rearrangement. An individual synthesis of product **B** was

Scheme 4. Possible Hydrogen Atom Abstraction Pathway through the L_1CuO_2 Adduct and Products A and B of HL_1 Degradation

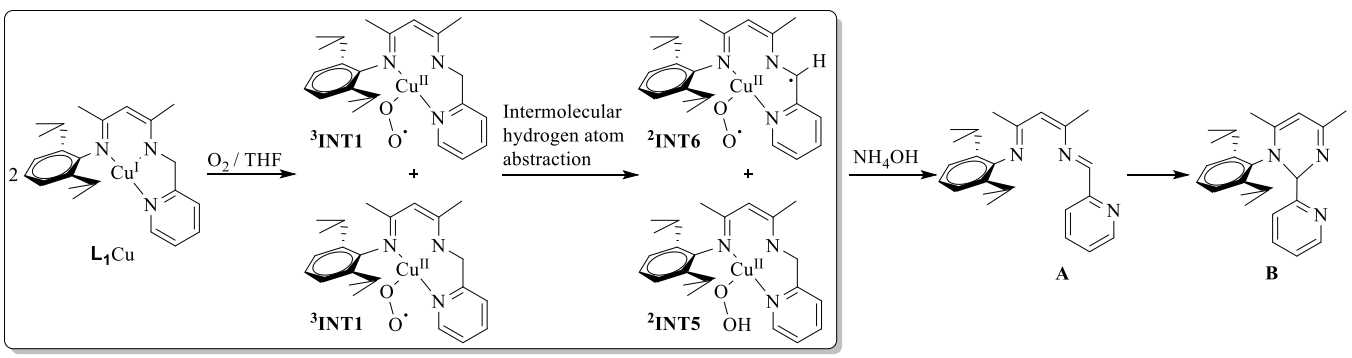

https://doi.org/10.1021/acsomega.3c02004
ACS Omega 2023, 8, 21096−21106

Scheme 5. Possible Pathway for Reactivity Study of Copper Complex L_2Cu with O_2

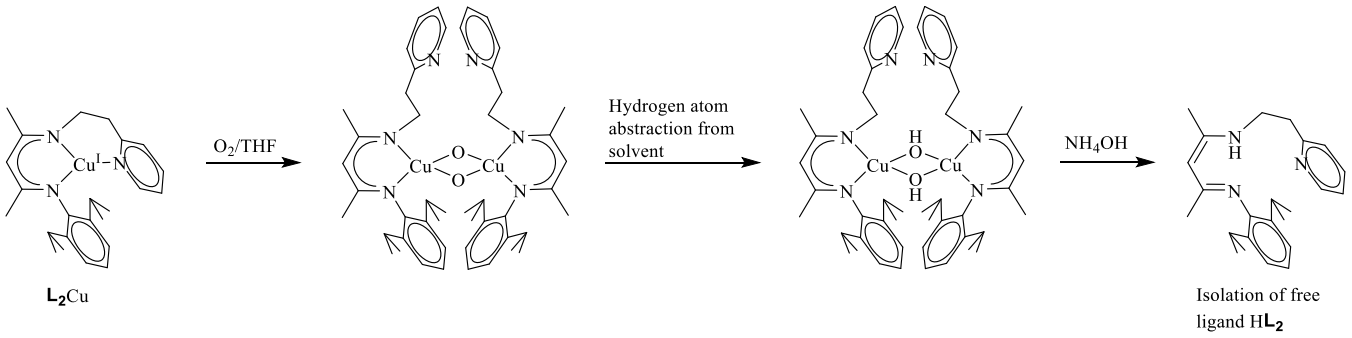

reported and also confirmed from dianion species of *N*-aryl-*N*′-alkyl unsymmetrical *β*-diketiminate generated via double deprotonation by potassium benzoyl and then oxidated by 2 equivalents of ferrocenium. Wolczanski et al. proposed that diimine **A** should be a reasonable intermediate during **B** formation.[58] Indeed, **A** was isolated as a ligand in complex $[\mathbf{A}Fe(CO)_2]$ via CO-induced and iron-mediated C−H activation of *N*-aryl-*N*′-alkyl unsymmetrical *β*-diketiminato ligand without rearrangement.[58] In the case of the $\mathbf{L_1}Cu$ ligand degradation study in the presence of NH_4OH, we can isolate the higher yield of un-complexation products **A** and **B**, which both are confirmed by ^1H NMR.

On the other hand, the pathway of the dioxygen activation of $\mathbf{L_2}Cu$ at −80 °C results in the formation of bis(*μ*-oxo) species, $[(\mathbf{L_2}Cu)_2(\mu\text{-}O_2)]$, with two uncoordinated pendant pyridyl arms (Scheme 5), which will further undergo hydrogen atom abstraction from the solvent and then lead to the formation of the bis(*μ*-hydroxide) product $[(\mathbf{L_2}Cu)_2(\mu\text{-}OH_2)]$[40] due to the thermally unstable nature of bis(*μ*-oxo)copper species, which was well addressed.[8,59,60] The organic substance analysis study of $[(\mathbf{L_2}Cu)_2(\mu\text{-}O)_2]$ species with and without NH_4OH addition shows no ligand degradation product as free ligand $H\mathbf{L_2}$. The lack of ligand degradation results can be attributed to the presence of the pyridylethyl arm, which may not undergo hydrogen atom abstraction as easily as the more reactive methylene group present in the pyridylmethyl arm of the $[(\mu\text{-}\mathbf{L_1})_2(CuO_2)_2]$ species.

CONCLUSIONS

Herein, we report that the *N*-aryl-*N*′-methylpyridyl unsymmetrical *β*-diketiminato copper(I) complex in a 1:1 Cu/O_2 ratio results in the formation of mononuclear copper(III)-dioxygen $\mathbf{L_1}CuO_2$ ($\mathbf{L_1}$ = one carbon pyridyl arm) adducts, while the 2:1 Cu/O_2 ratio results in the formation of the *N*-aryl-*N*′-ethylpyridyl unsymmetrical *β*-diketiminato dinuclear copper(II)-dioxygen $[(\mathbf{L_2}Cu)_2(\mu\text{-}O)_2]$ ($\mathbf{L_2}$ = two carbon pyridyl arm) adduct, as confirmed by the spectroscopic studies such as UV−vis and EPR. Furthermore, the 1:1 Cu/O_2 ratio of $\mathbf{L_1}CuO_2$ species will undergo intermolecular C−H activation on the pyridylmethyl arm to form **A** in the presence of NH_4OH as a demetallation agent and **A** will further undergo intramolecular rearrangement to form **B**. Products **A** and **B** were confirmed by ^1H-NMR and ESI-MS. Meanwhile, the two carbon pyridyl arm dinuclear copper(II)-dioxygen adduct of $[(\mathbf{L_2}Cu)_2(\mu\text{-}O)_2]$ shows no ligand degradation product on the supporting ligand, which suggests the reactivity difference between pyridylmethyl and pyridylethyl arms of *N*-aryl-*N*′-alkylpyridyl unsymmetrical *β*-diketiminato copper dioxygen adducts.

EXPERIMENTAL SECTION

General Considerations. All manipulations involving oxygenation studies of copper(I) complexes $\mathbf{L_1}Cu$ and $\mathbf{L_2}Cu$ were carried out under an inert N_2 atmosphere of the glove box. The copper(I) complexes $\mathbf{L_1}Cu$ and $\mathbf{L_2}Cu$ and *N*-aryl-*N*′-alkylpyridyl *β*-diketiminato ligands $\mathbf{L_1}H$ and $\mathbf{L_2}H$ were prepared by following published procedures.[40,41,57] Chemical reagents were purchased from Aldrich Chemical Co. Ltd., Lancaster Chemicals Ltd., or Fluka Ltd. All reagents were used without further purification. All solvents like THF, toluene, Et_2O, hexanes, and pentanes used in the experiments were passed through solvent purification columns and then degassed. ^1H NMR and ^{13}C NMR spectra were recorded using JEOL 400 MHz NMR instruments. UV−vis spectra were recorded on an Agilent 8453 diode array spectrophotometer. Low-temperature spectra had been accomplished by employing the system of a Unisoku low-temperature UV−vis cell holder. Electrospray ionization mass spectrometry spectra were recorded on a Waters ZQ 4000 mass spectrometer. High-resolution mass spectra (HRMS) were measured with a mass spectrometer Finnigan/Thermo Quest MAT 95XL. All GC−MS experiments were conducted on a Thermo Finnigan (TRACEGC - POLARISQ) GC system. The GC column was a GsBP-5 ms with dimensions 30 m × 0.25 mm × 0.50 *μ*m. The standard method used for all runs involved an initial oven temperature of 50 °C (held for 0−2 min.), followed by a 10 °C/ min. ramp to 280 °C that was held for 25 min.

Low-Temperature Oxygenation of $\mathbf{L_1}Cu$ and $\mathbf{L_2}Cu$. *UV−vis Spectroscopy.* In a typical experiment, a solution of $\mathbf{L_1}Cu$ and $\mathbf{L_2}Cu$ in THF (1 mM) was placed in a UV cell under an inert atmosphere inside the glove box. A septum-sealed quartz cuvette was brought out of the glovebox and cooled to −80 °C, and dry steam of O_2 was bubbled through the solution for ∼100 s. The solution of $\mathbf{L_1}Cu$ and $\mathbf{L_2}Cu$ showed a color change from reddish to yellow and UV−vis signal at 600−800 nm. The excess of O_2 was removed by continuous nitrogen purge for 30 min, which will not affect the final spectrum. Then the solution was warmed up to 25 °C, resulting in the disappearance of the peak around 350−600 nm. After warming to 25 °C, color change was observed from yellow to green.

Spectrophotometric O_2 Titrations. The experiment procedure at −80 °C mentioned here follows the details as reported in the literature.[2,8,59,61,62] A 4 mL sample of stock solution of $\mathbf{L_1}Cu$ and $\mathbf{L_2}Cu$ in THF (0.175 mM) was placed in a 0.2 cm path length UV−vis cuvette and cooled to −80 °C. Spectra were taken before and after to ensure that no sample

https://doi.org/10.1021/acsomega.3c02004
ACS Omega 2023, 8, 21096−21106

degradation had occurred. The O_2–saturated THF solution (10 mM)[59] was prepared by bubbling the dry O_2 gas through nitrogen-saturated THF in a 25 mL round bottom flask at 25 °C for 30 min. During titration, 0.1 equivalent, that is, 7 μL of O_2 saturated THF solution each is required to inject into the cuvette containing the solution of $\mathbf{L_1}$Cu and $\mathbf{L_2}$Cu (0.175 mM), where it was left to equilibrate with stirring. The progress of oxygenation was followed by monitoring of the absorption band at 350 nm ($\mathbf{L_1}$Cu) or 420 nm ($\mathbf{L_2}$Cu) in the UV−vis spectrum until no further increase in the absorbance was observed. The Cu/O_2 stoichiometry was calculated from one ($\mathbf{L_1}$Cu) or two ($\mathbf{L_2}$Cu) replicates run.

Hydroxylation Study of L_1Cu. $\mathbf{L_1}$Cu (100 mg, 0.270 mmol) was dissolved into deaerated THF (10 mL) under anaerobic conditions at room temperature, and then the solution was cooled to −80 °C and bubbled with O_2 for 30 min. The green color reaction mixture was taken slowly from −80 to 25 °C for 1.5 h, and then $NH_4OH_{(aq)}$ (3.3 mL, ∼100 equivalents) was added and stirred for 30 min or 2 h. A significant color change was observed from dark green to reddish brown after the addition of $NH_4OH_{(aq)}$. Reddish-brown color compounds in the organic layer (3.3 mL) and blue color solution in the aqueous layer (10 mL) were obtained, followed by extraction with diethyl ether resulting in the formation of product **A** (30 min) and product **B** (2 h), respectively.

*Product **A**.* ^{1}H NMR (C_6D_6, 400 MHz, 298 K): δ 8.44 (d, J = 5 Hz, 1H, a), 7.61 (m, 1H, c), 7.10 (m, 3H, d, b, k), 6.93 (m, 1H, i), 6.56 (td, 1H, j), 6.32 (s, 1H, e), 5.07 (s, 1H, g), 3.44 (sp, J = 7 Hz, 2H, o, l), 2.04 (s, 3H, f), 1.52 (s, 3H, h), 1.35 (d, J = 7 Hz, 3H, p), 1.15 (d, J = 7 Hz, 3H, q), 1.06 (d, J = 7 Hz, 3H, n), 0.56 (d, J = 7 Hz, 3H, m). ^{13}C{^{1}H} NMR (C_6D_6, 100.06 MHz, 298 K): δ 167.17, 160.76, 156.03, 149.98, 147.68, 138.58, 136.63, 123.85, 123.63, 122.11, 120.73, 95.35, 49.42, 28.92, 24.50, 23.51, 22.13, 19.46. GC−MS: 348.24. HRMS (ESI-TOF) m/z: $[M + H]^+$ calcd for $C_{23}H_{20}N_3$, 348.2434; found, 348.2432.

*Product **B**.* ^{1}H NMR (C_6D_6, 400 MHz, 298 K): δ 8.42 (d, J = 5 Hz, 1H, a), 7.53 (m, 2H, c, d), 7.09 (m, 1H, b), 7.01 (m, 2H, k, i), 6.93 (m, 1H, j), 5.86 (s, 1H, e), 5.03 (s, 1H, g), 3.13 (sp, J = 7 Hz, 1H, o), 2.96 (sp, J = 7 Hz, 1H, l), 1.96 (s, 3H, f), 1.60 (s, 3H, h), 1.23 (d, J = 7 Hz, 3H, p), 1.09 (d, J = 7 Hz, 3H, q), 0.98 (d, J = 7 Hz, 3H, n), 0.29 (d, J = 7 Hz, 3H, m). ^{13}C{^{1}H} NMR (C_6D_6, 100.06 MHz, 298 K): δ 161.78, 159.74, 151.24, 148.16, 147.88, 146.58, 137.74, 135.61, 127.45, 123.88, 123.18, 122.01, 121.34, 95.02, 82.75, 26.95, 26.87, 23.82, 23.39, 23.16, 23.07, 22.97, 19.15. GC−MS: 348.24. HRMS (ESI-TOF) m/z: $[M + H]^+$ calcd for $C_{23}H_{20}N_3$, 348.2434; found, 348.2432.

Hydroxylation Study of L_2Cu. $\mathbf{L_2}$Cu (100 mg, 0.261 mmol) was dissolved into deaerated THF (10 mL) under anaerobic conditions at room temperature, and then the solution was cooled to −80 °C and bubbled with O_2 for 30 min. A mixture of organic compounds (3.2 mL) and blue color solution in an aqueous layer (10 mL) was obtained after an ordinary workup treatment of reaction mixture with NH_4OHaq (3.2 mL, ∼100 equivalents) and following extraction by diethyl ether to give a product of $H\mathbf{L_2}$.

Procedures for the Reaction of L_1CuCl with KO_2. All handling of potassium superoxide was performed in a septum-sealed Schlenk flask under nitrogen. Potassium superoxide solutions were prepared by placing 1 equivalent of KO_2 and 1.1 equivalents of 18-crown-6 in a scintillation vial and dissolving in DMF to a desired concentration. The mixture was magnetically stirred for a minimum of 10 min at room temperature, generating a fine suspension in a slightly yellow solution. In a typical UV−vis monitored reaction with excess KO_2, 1.5 mL of a stock solution of KO_2/18-crown-6 in DMF (10 mM) was placed in a UV/vis cuvette and diluted with 1 mL of THF. After cooling the cuvette to −80 °C, 0.5 mL of a stock solution of $\mathbf{L_1}$CuCl in THF (0.175 mM) was added and the reaction was monitored by UV−vis spectroscopy.

Procedures for the Reaction of L_2CuCl with H_2O_2/Et_3N. All handling of hydrogen peroxide was performed in a septum-sealed Schlenk flask under nitrogen. Hydrogen peroxide solutions were prepared by placing 1 equivalent of H_2O_2 (50 wt %) and 2 equivalents of Et_3N in a scintillation vial. In a typical UV−vis monitored reaction, 1.5 mL of a stock solution of H_2O_2/Et_3N in THF (10 mM) was placed in a UV/vis cuvette. After cooling the cuvette to −80 °C, 0.5 mL of a stock solution of $\mathbf{L_2}$CuCl in THF (0.175 mM) was added and the reaction was monitored by UV−vis spectroscopy.

Independent Synthesis of (2*E*,3*Z*)-*N*-(2,6-Diisopropylphenyl)-4-(((*E*)-pyridin-2-ylmethylene)amino)pent-3-en-2-imine (Product A). 2-pyridine carboxaldehyde (500 mg, 1.93 mmol) was added to an ethanolic solution of amine (2.06 mL, 1.93 mmol) in the presence of 5 Å molecular sieves, and the mixtures were heated under reflux for 6 h. The mixture was filtered to remove 5 Å molecular sieves and washed with CH_2Cl_2 (20 mL). The resultant solution was dried with $MgSO_4$ and evaporated under reduced pressure. The product was obtained via vacuum distillation. The confirmation of the product has been done by ^{1}H NMR, ^{13}C{^{1}H}NMR, and UV−vis spectroscopy, which is consistent with product **A**.

Conversion of Product A to B. Product **A** (10 mg, 0.02 mmol) was dissolved in d-benzene and taken in an NMR tube. 0.5 equivalents of NH_4OH (0.35 mL, 0.01 mmol) was added, and the reaction was monitored from 30 min to 2 h. A significant change in the NMR peaks confirms the conversion of product **A** to **B**. The confirmation of product **B** has been done by ^{1}H NMR and UV−vis spectroscopy.

■ ASSOCIATED CONTENT

Supporting Information

The Supporting Information is available free of charge at https://pubs.acs.org/doi/10.1021/acsomega.3c02004.

Copper dioxygen adduct characterization data with UV−vis, EPR, and ^{1}H NMR spectral product analysis (PDF)

■ AUTHOR INFORMATION

Corresponding Authors

Hsing-Yin Chen − *Department of Medicinal and Applied Chemistry, Kaohsiung Medical University, Kaohsiung 807, Taiwan;* orcid.org/0000-0003-3948-8915; Email: hychen@kmu.edu.tw

Sodio C. N. Hsu − *Department of Medicinal and Applied Chemistry, Kaohsiung Medical University, Kaohsiung 807, Taiwan; Department of Chemistry, National Sun Yat-Sen University, Kaohsiung 804, Taiwan; Department of Medical Research, Kaohsiung Medical University Hospital, Kaohsiung 807, Taiwan;* orcid.org/0000-0002-2576-7289; Email: sodiohsu@kmu.edu.tw

https://doi.org/10.1021/acsomega.3c02004
ACS Omega 2023, 8, 21096−21106

Authors

Kuldeep Chand − *Department of Medicinal and Applied Chemistry, Kaohsiung Medical University, Kaohsiung 807, Taiwan;* orcid.org/0000-0001-6666-7543

Naorem Jemes Meitei − *Department of Medicinal and Applied Chemistry, Kaohsiung Medical University, Kaohsiung 807, Taiwan;* orcid.org/0000-0002-8765-2495

Yu-Lun Chang − *Department of Medicinal and Applied Chemistry, Kaohsiung Medical University, Kaohsiung 807, Taiwan; Department of Chemistry, National Sun Yat-Sen University, Kaohsiung 804, Taiwan*

Cheng-Long Tsai − *Department of Medicinal and Applied Chemistry, Kaohsiung Medical University, Kaohsiung 807, Taiwan*

Complete contact information is available at: https://pubs.acs.org/10.1021/acsomega.3c02004

Author Contributions

This manuscript was written through contributions of all authors and have given approval to this final version of manuscript.

Notes

The authors declare no competing financial interest.

■ ACKNOWLEDGMENTS

This research was supported by the Ministry of Science and Technology, Taiwan (MOST 111-2113-M-037-006). The NSYSU-KMU Joint Research Project (NSYSUKMU 108-I002) and the Kaohsiung Medical University (Grant No. KMU-DK(B)110001). We thank the Center for Research Resources and Development of KMU for use their facilities.

■ REFERENCES

(1) Lee, J. Y.; Peterson, R. L.; Ohkubo, K.; Garcia-Bosch, I.; Himes, R. A.; Woertink, J.; Moore, C. D.; Solomon, E. I.; Fukuzumi, S.; Karlin, K. D. Mechanistic Insights into the Oxidation of Substituted Phenols via Hydrogen Atom Abstraction by a Cupric−Superoxo Complex. *J. Am. Chem. Soc.* **2014**, *136*, 9925−9937.

(2) Gupta, A. K.; Tolman, W. B. Cu(I)/O_2 chemistry using a β-diketiminate supporting ligand derived from N,N-dimethylhydrazine: a $[Cu_3O_2]^{3+}$ complex with novel reactivity. *Inorg. Chem.* **2012**, *51*, 1881−1888.

(3) Abe, T.; Morimoto, Y.; Tano, T.; Mieda, K.; Sugimoto, H.; Fujieda, N.; Ogura, T.; Itoh, S. Geometric Control of Nuclearity in Copper(I)/Dioxygen Chemistry. *Inorg. Chem.* **2014**, *53*, 8786−8794.

(4) Aboelella, N. W.; Gherman, B. F.; Hill, L. M.; York, J. T.; Holm, N.; Young, V. G., Jr.; Cramer, C. J.; Tolman, W. B. Effects of Thioether Substituents on the O_2 Reactivity of β-Diketiminate−Cu(I) Complexes: Probing the Role of the Methionine Ligand in Copper Monooxygenases. *J. Am. Chem. Soc.* **2006**, *128*, 3445−3458.

(5) Garcia-Bosch, I.; Cowley, R. E.; Diaz, D. E.; Peterson, R. L.; Solomon, E. I.; Karlin, K. D. Substrate and Lewis Acid Coordination Promote O−O Bond Cleavage of an Unreactive $L_2Cu^{II}_2(O_2^{2-})$ Species to Form $L_2Cu^{III}_2(O)_2$ Cores with Enhanced Oxidative Reactivity. *J. Am. Chem. Soc.* **2017**, *139*, 3186−3195.

(6) Elwell, C. E.; Gagnon, N. L.; Neisen, B. D.; Dhar, D.; Spaeth, A. D.; Yee, G. M.; Tolman, W. B. Copper−Oxygen Complexes Revisited: Structures, Spectroscopy, and Reactivity. *Chem. Rev.* **2017**, *117*, 2059−2107.

(7) Kunishita, A.; Ertem, M. Z.; Okubo, Y.; Tano, T.; Sugimoto, H.; Ohkubo, K.; Fujieda, N.; Fukuzumi, S.; Cramer, C. J.; Itoh, S. Active Site Models for the Cu_A Site of Peptidylglycine α-Hydroxylating Monooxygenase and Dopamine β-Monooxygenase. *Inorg. Chem.* **2012**, *51*, 9465−9480.

(8) Spencer, D. J.; Reynolds, A. M.; Holland, P. L.; Jazdzewski, B. A.; Duboc-Toia, C.; Le Pape, L.; Yokota, S.; Tachi, Y.; Itoh, S.; Tolman, W. B. Copper Chemistry of β-Diketiminate Ligands: Monomer/Dimer Equilibria and a New Class of Bis(μ-oxo) dicopper Compounds. *Inorg. Chem.* **2002**, *41*, 6307−6321.

(9) Donoghue, P. J.; Gupta, A. K.; Boyce, D. W.; Cramer, C. J.; Tolman, W. B. An Anionic, Tetragonal Copper(II) Superoxide Complex. *J. Am. Chem. Soc.* **2010**, *132*, 15869−15871.

(10) Lanci, M. P.; Smirnov, V. V.; Cramer, C. J.; Gauchenova, E. V.; Sundermeyer, J.; Roth, J. P. Isotopic probing of molecular oxygen activation at copper(I) sites. *J. Am. Chem. Soc.* **2007**, *129*, 14697−14709.

(11) Komiyama, K.; Furutachi, H.; Nagatomo, S.; Hashimoto, A.; Hayashi, H.; Fujinami, S.; Suzuki, M.; Kitagawa, T. Dioxygen Reactivity of Copper(I) Complexes with Tetradentate Tripodal Ligands Having Aliphatic Nitrogen Donors: Synthesis, Structures, and Properties of Peroxo and Superoxo Complexes. *Bull. Chem. Soc. Jpn.* **2004**, *77*, 59−72.

(12) Jazdzewski, B. A.; Reynolds, A. M.; Holland, P. L.; Young, V. G.; Kaderli, S.; Zuberbühler, A. D.; Tolman, W. B. Copper(I)-phenolate complexes as models of the reduced active site of galactose oxidase: synthesis, characterization, and O_2 reactivity. *J. Biol. Inorg. Chem.* **2003**, *8*, 381−393.

(13) Maiti, D.; Lee, D. H.; Gaoutchenova, K.; Würtele, C.; Holthausen, M. C.; Narducci Sarjeant, A. A.; Sundermeyer, J.; Schindler, S.; Karlin, K. D. Reactions of a Copper(II) Superoxo Complex Lead to C-H and O-H Substrate Oxygenation: Modeling Copper-Monooxygenase C-H Hydroxylation. *Angew. Chem., Int. Ed.* **2008**, *120*, 88−91.

(14) Maiti, D.; Fry, H. C.; Woertink, J. S.; Vance, M. A.; Solomon, E. I.; Karlin, K. D. A 1:1 Copper−Dioxygen Adduct is an End-on Bound Superoxo Copper(II) Complex which Undergoes Oxygenation Reactions with Phenols. *J. Am. Chem. Soc.* **2007**, *129*, 264−265.

(15) Würtele, C.; Gaoutchenova, E.; Harms, K.; Holthausen, M. C.; Sundermeyer, J.; Schindler, S. Crystallographic Characterization of a Synthetic 1:1 End-On Copper Dioxygen Adduct Complex. *Angew. Chem., Int. Ed.* **2006**, *45*, 3867−3869.

(16) Schatz, M.; Raab, V.; Foxon, S. P.; Brehm, G.; Schneider, S.; Reiher, M.; Holthausen, M. C.; Sundermeyer, J.; Schindler, S. Combined Spectroscopic and Theoretical Evidence for a Persistent End-On Copper Superoxo Complex. *Angew. Chem., Int. Ed.* **2004**, *43*, 4360−4363.

(17) Thiabaud, G.; Guillemot, G.; Schmitz-Afonso, I.; Colasson, B.; Reinaud, O. Solid-State Chemistry at an Isolated Copper(I) Center with O_2. *Angew. Chem. Int. Ed.* **2009**, *121*, 7519−7522.

(18) Izzet, G.; Zeitouny, J.; Akdas-Killig, H.; Frapart, Y.; Ménage, S.; Douziech, B.; Jabin, I.; Le Mest, Y.; Reinaud, O. Dioxygen Activation at a Mononuclear Cu(I) Center Embedded in the Calix[6]arene-Tren Core. *J. Am. Chem. Soc.* **2008**, *130*, 9514−9523.

(19) Decker, H.; Schweikardt, T.; Nillius, D.; Salzbrunn, U.; Jaenicke, E.; Tuczek, F. Similar enzyme activation and catalysis in hemocyanins and tyrosinases. *Gene* **2007**, *398*, 183−191.

(20) Decker, H.; Schweikardt, T.; Tuczek, F. The First Crystal Structure of Tyrosinase: All Questions Answered? *Angew. Chem., Int. Ed.* **2006**, *45*, 4546−4550.

(21) Trammell, R.; Rajabimoghadam, K.; Garcia-Bosch, I. Copper-Promoted Functionalization of Organic Molecules: from Biologically Relevant Cu/O_2 Model Systems to Organometallic Transformations. *Chem. Rev.* **2019**, *119*, 2954−3031.

(22) Mirica, L. M.; Ottenwaelder, X.; Stack, T. D. P. Structure and Spectroscopy of Copper−Dioxygen Complexes. *Chem. Rev.* **2004**, *104*, 1013−1046.

(23) Czaikowski, M. E.; McNeece, A. J.; Boyn, J.-N.; Jesse, K. A.; Anferov, S. W.; Filatov, A. S.; Mazziotti, D. A.; Anderson, J. S. Generation and Aerobic Oxidative Catalysis of a Cu(II) Superoxo Complex Supported by a Redox-Active Ligand. *J. Am. Chem. Soc.* **2022**, *144*, 15569−15580.

(24) Keown, W.; Gary, J. B.; Stack, T. D. High-valent copper in biomimetic and biological oxidations. *J. Biol. Inorg. Chem.* **2017**, *22*, 289−305.
(25) Rolff, M.; Schottenheim, J.; Tuczek, F. Monooxygenation of external phenolic substrates in small-molecule dicopper complexes: implications on the reaction mechanism of tyrosinase. *J. Coord. Chem.* **2010**, *63*, 2382−2399.
(26) Rolff, M.; Schottenheim, J.; Decker, H.; Tuczek, F. Copper−O_2 reactivity of tyrosinase models towards external monophenolic substrates: molecular mechanism and comparison with the enzyme. *Chem. Soc. Rev.* **2011**, *40*, 4077−4098.
(27) Schneider, R.; Engesser, T. A.; Hamann, J. N.; Näther, C.; Tuczek, F. Dinuclear Copper(I) Complexes Supported by Bis-Tridentate N-Donor-Ligands: Turning-On Tyrosinase Activity. *Eur. J. Inorg. Chem.* **2022**, *2022*, No. e202200509.
(28) Kim, S.; Ginsbach, J. W.; Billah, A. I.; Siegler, M. A.; Moore, C. D.; Solomon, E. I.; Karlin, K. D. Tuning of the Copper−Thioether Bond in Tetradentate N_3S (thioether) Ligands; O−O Bond Reductive Cleavage via a $[Cu^{II}_2$ (μ-1, 2-peroxo)$]^{2+}/[Cu^{III}_2$ (μ-oxo)$_2]^{2+}$ Equilibrium. *J. Am. Chem. Soc.* **2014**, *136*, 8063−8071.
(29) Aboelella, N. W.; Lewis, E. A.; Reynolds, A. M.; Brennessel, W. W.; Cramer, C. J.; Tolman, W. B. Snapshots of dioxygen activation by copper: the structure of a 1: 1 Cu/O_2 adduct and its use in syntheses of asymmetric bis (μ-oxo) complexes. *J. Am. Chem. Soc.* **2002**, *124*, 10660−10661.
(30) Reynolds, A. M.; Gherman, B. F.; Cramer, C. J.; Tolman, W. B. Characterization of a 1:1 Cu−O_2 Adduct Supported by an Anilido Imine Ligand. *Inorg. Chem.* **2005**, *44*, 6989−6997.
(31) Spencer, D. J.; Aboelella, N. W.; Reynolds, A. M.; Holland, P. L.; Tolman, W. B. β-Diketiminate Ligand Backbone Structural Effects on $Cu(I)/O_2$ Reactivity: Unique Copper−Superoxo and Bis(μ-oxo) Complexes. *J. Am. Chem. Soc.* **2002**, *124*, 2108−2109.
(32) Cramer, C. J.; Gour, J. R.; Kinal, A.; Włoch, M.; Piecuch, P.; Moughal Shahi, A. R.; Gagliardi, L. Stereoelectronic Effects on Molecular Geometries and State-Energy Splittings of Ligated Monocopper Dioxygen Complexes. *J. Phys. Chem. A* **2008**, *112*, 3754−3767.
(33) Oguadinma, P. O.; Schaper, F. Syntheses and structures of bis(2,6-xylyl-nacnac) copper(I) complexes. *Inorg. Chim. Acta* **2009**, *362*, 570−574.
(34) Park, K.-H.; Bradley, A. Z.; Thompson, J. S.; Marshall, W. J. Nonfluorinated Volatile Copper(I) 1,3-Diketiminates as Precursors for Cu Metal Deposition via Atomic Layer Deposition. *Inorg. Chem.* **2006**, *45*, 8480−8482.
(35) Thompson, J. S.; Bradley, A. Z.; Park, K.-H.; Dobbs, K. D.; Marshall, W. Copper(I) Complexes with Bis(trimethylsilyl)acetylene: Role of Ancillary Ligands in Determining π Back-Bonding Interactions. *Organometallics* **2006**, *25*, 2712−2714.
(36) Cramer, C. J.; Tolman, W. B. Mononuclear Cu−O_2 Complexes: Geometries, Spectroscopic Properties, Electronic Structures, and Reactivity. *Acc. Chem. Res.* **2007**, *40*, 601−608.
(37) Aboelella, N. W.; Kryatov, S. V.; Gherman, B. F.; Brennessel, W. W.; Young, V. G.; Sarangi, R.; Rybak-Akimova, E. V.; Hodgson, K. O.; Hedman, B.; Solomon, E. I. Dioxygen Activation at a Single Copper Site: Structure, Bonding, and Mechanism of Formation of 1:1 Cu−O_2 Adducts. *J. Am. Chem. Soc.* **2004**, *126*, 16896−16911.
(38) Hill, L. M.; Gherman, B. F.; Aboelella, N. W.; Cramer, C. J.; Tolman, W. B. Electronic tuning of β-diketiminate ligands with fluorinated substituents: effects on the O_2-reactivity of mononuclear Cu(I) complexes. *Dalton Trans.* **2006**, 4944−4953.
(39) Reynolds, A. M.; Lewis, E. A.; Aboelella, N. W.; Tolman, W. B. Reactivity of a 1:1 copper−oxygen complex: isolation of a Cu(II)-o-iminosemiquinonato species. *Chem. Commun.* **2005**, 2014−2016.
(40) Chuang, W. J.; Hsu, S. P.; Chand, K.; Yu, F. L.; Tsai, C. L.; Tseng, Y. H.; Lu, Y. H.; Kuo, J. Y.; Carey, J. R.; Chen, H. Y.; Chen, H. Y.; Chiang, M. Y.; Hsu, S. C. Reactivity Study of Unsymmetrical β-Diketiminato Copper(I) Complexes: Effect of the Chelating Ring. *Inorg. Chem.* **2017**, *56*, 2722−2735.
(41) Chuang, W.-J.; Chen, H.-Y.; Chen, W.-T.; Chang, H.-Y.; Chiang, M. Y.; Chen, H.-Y.; Hsu, S. C. Steric and chelating ring concerns on the l-lactide polymerization by asymmetric β-diketiminato zinc complexes. *RSC Adv.* **2016**, *6*, 36705−36714.
(42) Chand, K.; Chu, Y.-C.; Wang, T.-W.; Kao, C.-L.; Lin, Y.-F.; Tsai, M.-L.; Hsu, S. C. Nitric oxide generation study of unsymmetrical β-diketiminato copper (II) nitrite complexes. *Dalton Trans.* **2022**, *51*, 3485−3496.
(43) Osako, T.; Nagatomo, S.; Tachi, Y.; Kitagawa, T.; Itoh, S. Low-Temperature Stopped-Flow Studies on the Reactions of Copper(II) Complexes and H_2O_2: The First Detection of a Mononuclear Copper(II)−Peroxo Intermediate. *Angew. Chem. Int. Ed.* **2002**, *114*, 4501−4504.
(44) Kobayashi, Y.; Ohkubo, K.; Nomura, T.; Kubo, M.; Fujieda, N.; Sugimoto, H.; Fukuzumi, S.; Goto, K.; Ogura, T.; Itoh, S. Copper(I)-Dioxygen Reactivity in a Sterically Demanding Tripodal Tetradentate tren Ligand: Formation and Reactivity of a Mononuclear Copper(II) End-On Superoxo Complex. *Eur. J. Inorg. Chem.* **2012**, *2012*, 4574−4578.
(45) Kim, S.; Lee, J. Y.; Cowley, R. E.; Ginsbach, J. W.; Siegler, M. A.; Solomon, E. I.; Karlin, K. D. A N3S(thioether)-Ligated CuII-Superoxo with Enhanced Reactivity. *J. Am. Chem. Soc.* **2015**, *137*, 2796−2799.
(46) Fujisawa, K.; Tanaka, M.; Moro-oka, Y.; Kitajima, N. A monomeric side-on superoxocopper (II) complex: Cu (O_2)(HB(3-^{t}Bu-5-^{i}Prpz)$_3$). *J. Am. Chem. Soc.* **1994**, *116*, 12079−12080.
(47) Paria, S.; Morimoto, Y.; Ohta, T.; Okabe, S.; Sugimoto, H.; Ogura, T.; Itoh, S. Copper (I)−Dioxygen Reactivity in the Isolated Cavity of a Nanoscale Molecular Architecture. *Eur. J. Inorg. Chem.* **2018**, *2018*, 1976−1983.
(48) Kunishita, A.; Kubo, M.; Sugimoto, H.; Ogura, T.; Sato, K.; Takui, T.; Itoh, S. Mononuclear copper (II)− superoxo complexes that mimic the structure and reactivity of the active centers of PHM and DβM. *J. Am. Chem. Soc.* **2009**, *131*, 2788−2789.
(49) Solomon, E. I.; Ginsbach, J. W.; Heppner, D. E.; Kieber-Emmons, M. T.; Kjaergaard, C. H.; Smeets, P. J.; Tian, L.; Woertink, J. S. Copper dioxygen (bio)inorganic chemistry. *Faraday Discuss.* **2011**, *148*, 11−39.
(50) Gomila, A.; Le Poul, N.; Kerbaol, J.-M.; Cosquer, N.; Triki, S.; Douziech, B.; Conan, F.; Le Mest, Y. Electrochemical behavior and dioxygen reactivity of tripodal dinuclear copper complexes linked by unsaturated rigid spacers. *Dalton Trans.* **2013**, *42*, 2238−2253.
(51) Tabuchi, K.; Ertem, M. Z.; Sugimoto, H.; Kunishita, A.; Tano, T.; Fujieda, N.; Cramer, C. J.; Itoh, S. Reactions of Copper(II)-Phenol Systems with O_2: Models for TPQ Biosynthesis in Copper Amine Oxidases. *Inorg. Chem.* **2011**, *50*, 1633−1647.
(52) Maiti, D.; Narducci Sarjeant, A. A.; Karlin, K. D. Copper−Hydroperoxo-Mediated N-Debenzylation Chemistry Mimicking Aspects of Copper Monooxygenases. *Inorg. Chem.* **2008**, *47*, 8736−8747.
(53) Lee, D.-H.; Hatcher, L. Q.; Vance, M. A.; Sarangi, R.; Milligan, A. E.; Narducci Sarjeant, A. A.; Incarvito, C. D.; Rheingold, A. L.; Hodgson, K. O.; Hedman, B.; Solomon, E. I.; Karlin, K. D. Copper(I) Complex O_2-Reactivity with a N_3S Thioether Ligand: a Copper−Dioxygen Adduct Including Sulfur Ligation, Ligand Oxygenation, and Comparisons with All Nitrogen Ligand Analogues. *Inorg. Chem.* **2007**, *46*, 6056−6068.
(54) Ohi, H.; Tachi, Y.; Itoh, S. Modeling the Mononuclear, Dinuclear, and Trinuclear Copper(I) Reaction Centers of Copper Proteins Using Pyridylalkylamine Ligands Connected to 1,3,5-Triethylbenzene Spacer. *Inorg. Chem.* **2006**, *45*, 10825−10835.
(55) Nasir, M. S.; Cohen, B. I.; Karlin, K. D. Mechanism of aromatic hydroxylation in a copper monooxygenase model system. 1,2-Methyl migrations and the NIH shift in copper chemistry. *J. Am. Chem. Soc.* **1992**, *114*, 2482−2494.
(56) Martin, J.; Langer, J.; Elsen, H.; Harder, S. Alkaline Earth Metal Imido Complexes with Doubly Deprotonated Amidine and β-Diketimine Ligands. *Eur. J. Inorg. Chem.* **2020**, *2020*, 3573−3579.

https://doi.org/10.1021/acsomega.3c02004
ACS Omega 2023, 8, 21096−21106

(57) Chand, K.; Tsai, C. L.; Chen, H. Y.; Ching, W. M.; Hsu, S. P.; Carey, J. R.; Hsu, S. C. Improved Synthesis of Unsymmetrical N-Aryl-N′-alkylpyridyl ß-Diketimines Using Molecular Sieves and their Lithium Complexes. *Eur. J. Inorg. Chem.* **2018**, *2018*, 1093−1098.
(58) Morris, W. D.; Wolczanski, P. T.; Sutter, J. R.; Meyer, K.; Cundari, T. R.; Lobkovsky, E. B. Iron and Chromium Complexes Containing Tridentate Chelates Based on Nacnac and Imino-and Methyl-Pyridine Components: Triggering C-X Bond Formation. *Inorg. Chem.* **2014**, *53*, 7467−7484.
(59) Hong, S.; Hill, L. M.; Gupta, A. K.; Naab, B. D.; Gilroy, J. B.; Hicks, R. G.; Cramer, C. J.; Tolman, W. B. Effects of Electron-Deficient *β*-Diketiminate and Formazan Supporting Ligands on Copper(I)-Mediated Dioxygen Activation. *Inorg. Chem.* **2009**, *48*, 4514−4523.
(60) Dai, X.; Warren, T. H. Dioxygen activation by a neutral *β*-diketiminato copper(I) ethylene complex. *Chem. Commun.* **2001**, 1998−1999.
(61) Battino, R.; Rettich, T. R.; Tominaga, T. The solubility of oxygen and ozone in liquids. *J. Phys. Chem. Ref. Data* **1983**, *12*, 163−178.
(62) Battino, R. *Oxygen and Ozone*; Battino, R., Ed.; Pergamon Press: NewYork, 1981; Vol. *7*.

https://doi.org/10.1021/acsomega.3c02004
ACS Omega 2023, 8, 21096−21106